Palaeogeography, Palaeoclimatology, Palaeoecology 414 (2014) 332–341

Contents lists available at ScienceDirect

Palaeogeography, Palaeoclimatology, Palaeoecology

journal homepage: www.elsevier.com/locate/palaeo

Multiproxy geochemical analysis of a Panthalassic margin record of the early Toarcian oceanic anoxic event (Toyora area, Japan)

David B. Kemp [a,*], Kentaro Izumi [b]

[a] Environment, Earth and Ecosystems, Open University, Walton Hall, Milton Keynes, MK7 6AA, UK
[b] Department of Earth and Planetary Science, University of Tokyo, 7-3-1 Hongo, Bunkyo-ku, Tokyo 113-0033, Japan

ARTICLE INFO

Article history:
Received 12 June 2014
Received in revised form 11 September 2014
Accepted 19 September 2014
Available online 28 September 2014

Keywords:
Toarcian
Geochemistry
Japan
Panthalassa
Anoxia
Palaeoclimate

ABSTRACT

The early Toarcian oceanic anoxic event (OAE) was a significant palaeoenvironmental perturbation that led to marked changes in ocean chemistry and climate, and which also had a long-lasting impact on marine ecosystems. The global significance of the event has been recognised from the widespread occurrence of a ~3–7‰ negative excursion in the carbon-isotope ($\delta^{13}C$) composition of marine organic and inorganic matter and terrestrial plant material. This feature of the event is indicative of a pronounced perturbation to the global carbon cycle; an inference further supported by widespread evidence for seawater deoxygenation and elevated rates of organic carbon burial. Nevertheless, the precise palaeoenvironmental impacts of this event from sections outside of the Boreal and Tethyan realms are uncertain. Here, we present the results of a multiproxy geochemical study of an expanded record of the early Toarcian event from the northwest Panthalassa Ocean margin exposed in southwest Japan (Toyora area, Yamaguchi prefecture). Our results indicate that in the studied succession, organic matter enrichment persisted through the early Toarcian event, but elemental redox proxies do not support persistent seawater anoxia. Analyses of terrigenously derived major and trace element abundances coupled with sedimentological observations reveal an increase in coarse-grained sediment close to the onset of a ~−4‰ excursion in $\delta^{13}C_{org}$, and coincident with an inferred increase in terrestrial organic matter flux. These observations are consistent with previously published evidence for a marked strengthening of hydrological cycling and increased runoff that occurred contemporaneously with abrupt warming at the onset of the carbon isotope event.

1. Introduction

The early Toarcian oceanic anoxic event (~182 Ma) represents one of the most significant palaeoenvironmental perturbations of the Phanerozoic, resulting in marked disruption to both the climate system and marine ecosystems. The event is associated in particular with the widespread, ostensibly global, deposition of organic-rich facies under reducing conditions (Jenkyns, 1988; Fig. 1A). Coeval with this evidence for seawater deoxygenation is associated evidence for abrupt seawater warming, an increase in continental weathering rates, enhanced rates of biotic turnover, atmospheric pCO_2 changes and ocean acidification (Bailey et al., 2003; Cohen et al., 2004; McElwain et al., 2005; Caswell et al., 2009; Trecalli et al., 2012; Danise et al., 2013). One of the most significant geochemical characteristics of the event is a marked negative excursion of ~3–7‰ in the $\delta^{13}C$ of marine organic matter, marine carbonate and terrestrial plant material (e.g. Hesselbo et al., 2000; Jenkyns et al., 2001; al-Suwaidi et al., 2010; Caruthers et al., 2011; Gröcke et al., 2011; Kafousia et al., 2011; Izumi et al., 2012). This feature has been attributed to a large-scale transfer of carbon-12 through the exogenic carbon cycle, possibly from methane hydrate dissociation or from carbon released thermogenically from organic matter sources (Hesselbo et al., 2000; Kemp et al., 2005; McElwain et al., 2005; Svensen et al., 2007). The presence of this carbon-isotope excursion in terrestrial plant material and biomarkers of higher plant origin demonstrates the influence of the event on the atmospheric CO_2 reservoir and, given the presumed brevity of this reservoir's mixing time, indicates that the event was global (Hesselbo et al., 2000, 2007; French et al., 2014). The global expression of the negative carbon isotope excursion has further been established through analysis of early Toarcian rocks in globally distributed palaeogeographic locations, including various localities of the Panthalassa Ocean (Al-Suwaidi et al., 2010; Mazzini et al., 2010; Caruthers et al., 2011; Gröcke et al., 2011; Izumi et al., 2012).

Despite these advances, geochemical data that have yielded evidence for enhanced continental weathering, seawater deoxygenation and palaeotemperature change in European sections are not common from locations outside of the Tethyan and Boreal realms. Notably, the precise effects of the early Toarcian event on the geochemistry of Panthalassa and the surrounding region are unclear. Here, a geochemical investigation of the early Toarcian event has been carried out on a section deposited on the northwestern margin of Panthalassa and now exposed in southwest Japan (Fig. 1). This section, deposited in a shallow

* Corresponding author. Tel.: +44 1908 858492.
E-mail address: david.kemp@open.ac.uk (D.B. Kemp).

http://dx.doi.org/10.1016/j.palaeo.2014.09.019

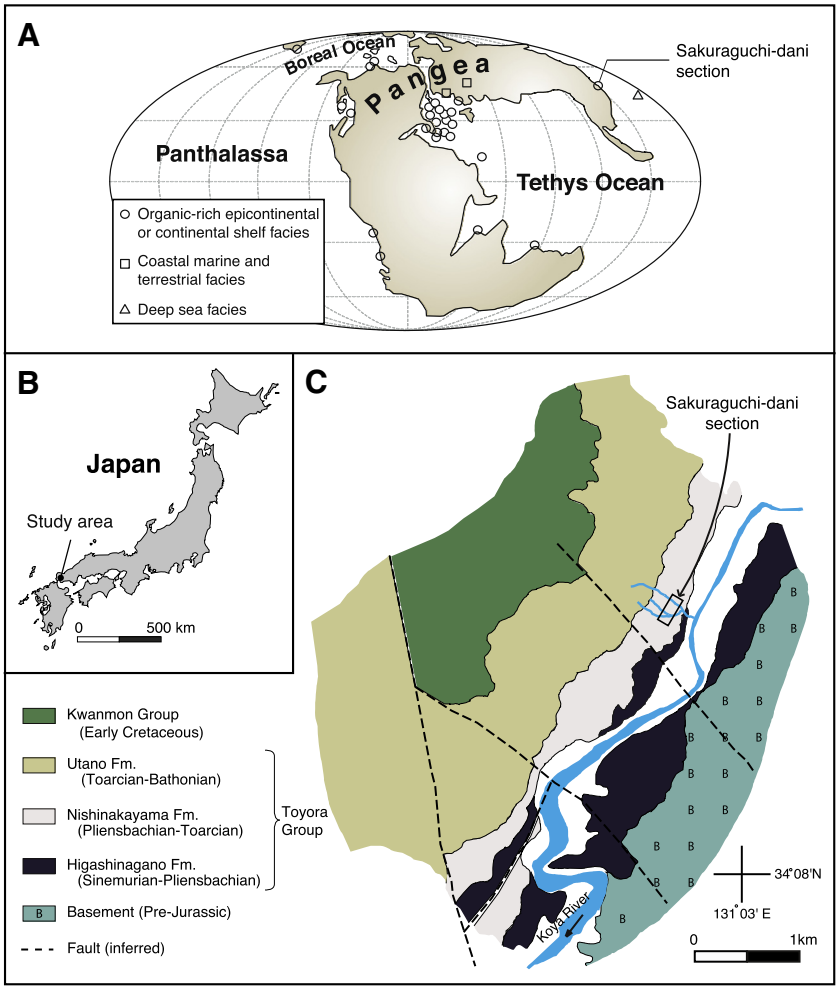

Fig. 1. A. Palaeogeographic map showing early Toarcian organic-rich deposits (redrawn from Izumi et al., 2012). The map highlights the European bias of existing studies, but also emphasizes the global nature of organic enrichment during the early Toarcian. B. Map of Japan showing location of studied Sakuraguchi-dani succession (Yamaguchi prefecture). C. Geological map of field area in the Tabe Basin (modified after Nakada and Matsuoka, 2011), with Sakuraguchi-dani area highlighted.

marine setting, has recently been shown by Izumi et al. (2012) to preserve a record of the early Toarcian negative $\delta^{13}C$ excursion spanning ~40 m. As such, this record of the event is the most expanded yet described from outside Europe, and thus suited to high-resolution study.

2. Geological setting and international correlation

Lower Jurassic siliciclastic sedimentary rocks of the Toyora Group crop out in the Toyora area of Yamaguchi prefecture (Fig. 1B) where these rocks form part of the fill of the Tabe Basin. In the northern part of the basin, the Nishinakayama Formation consists of Pliensbachian–Toarcian shallow marine silty shale, mudstone and fine-grained sandstone (Tanabe et al., 1982; Nakada and Matsuoka, 2011). Following Tanabe et al. (1982) and Izumi et al. (2012), this formation can be subdivided into three members: Na (silty shale, ~90 m thick), Nb (predominantly dark silty shale but with intercalated fine-grained sandstone and laminated, organic-rich shale, ~160 m thick), and Nc (alternating sandstone and mudstone, ~20–60 m thick) (Tanabe et al., 1982; Izumi et al., 2012). In the Sakuraguchi-dani valley of the Toyora area, the Nb member of the Nishinakayama Formation is relatively well exposed in mountainside ephemeral streambeds (Figs. 1C and 2). Izumi et al. (2012) logged a 90 m thick succession of the Nb member consisting of mudstone, siltstone, shale and fine-grained sandstone. Although not continuously exposed, $\delta^{13}C_{org}$ analysis through the succession by these authors indicated a ~4‰ negative excursion spanning ~40 m (Izumi et al., 2012). This record is readily interpreted as the early Toarcian event on the basis of the structure of the excursion and age constraints provided by a detailed ammonite biostratigraphy for the succession, correlable to Northern Europe (Izumi et al., 2012; Fig. 2). The biostratigraphic framework for the Tabe basin has a long history (e.g. Matsumoto and Ono, 1947; Hirano, 1973), and the latest refinements of Nakada and Matsuoka (2011) established three key ammonite zones within the Nb member of the Sakuraguchi-dani succession: the *Palparites paltus* Zone, the *Dactylioceras helianthoides* Zone, and the *Harpoceras inouyei* Zone (Nakada and Matsuoka, 2011; Fig. 2). Nakada and Matsuoka (2011), and subsequently Izumi et al. (2012), defined a correlation between this scheme and the Northern European standard (e.g. Page, 2003) that placed the base of the *P. paltus* Zone at the Pliensbachian–Toarcian boundary (i.e. base *Dactylioceras tenuicostatum* Zone of Northern Europe). *D. helianthoides* is known from the upper part of the *tenuicostatum* Zone of Northern Europe, as well as the *tenuicostatum* Subzone of southwest Panthalassa in Chile (Schmidt-Effing, 1972; Von Hillebrandt and Schmidt-Effing, 1981). These observations are broadly consistent with the position of the observed onset of the $\delta^{13}C_{org}$ excursion in both Japan and Europe, which is close to the first occurrence of *D. helianthoides* in the Sakuraguchi-dani section, and in the upper part of the *tenuicostatum* Zone of Yorkshire, UK (Fig. 2). Nakada and Matsuoka (2011) originally recognised the first occurrence of *H. inouyei* coeval with the first occurrence of *Cleviceras* cf. *exaratum* in the succession, and on this basis correlated this level with the base of the *Cleviceras exaratum* Subzone in Northern Europe. This correlation was refined by Izumi et al.

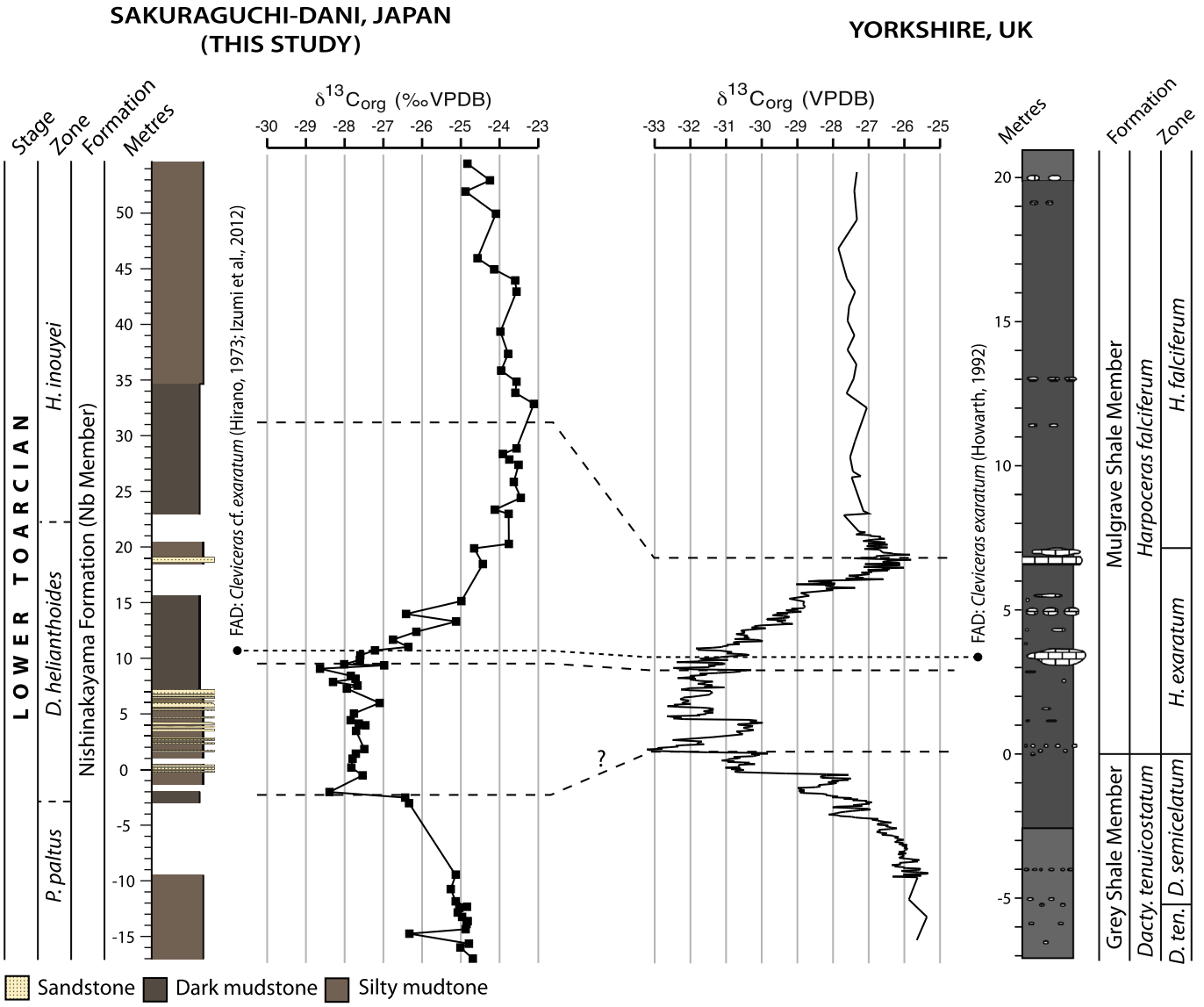

Fig. 2. Correlation of early Toarcian $\delta^{13}C_{org}$ excursions from Sakuraguchi-dani section and the Cleveland Basin of Yorkshire (UK) (Yorkshire data from Kemp et al. (2005) and Cohen et al. (2004). Log of Sakuraguchi-dani succession is based on Izumi et al. (2012) and our updated field observations. Dashed lines show correlation based on expression of $\delta^{13}C_{org}$ changes. Dotted line shows correlation based on first appearance datum (FAD) of *exaratum* ammonites.

(2012), who noted that the first occurrence of *C.* cf. *exaratum*, first described by Hirano (1973), actually occurs lower in the succession, close to where the $\delta^{13}C_{org}$ signal begins to recover to more positive values (Fig. 2). In the UK (Yorkshire) and Germany, the first occurrence of *C. exaratum* also occurs close to the point where $\delta^{13}C_{org}$ values begin a positive trend back toward background values (Howarth, 1992; Fig. 2). In Yorkshire, this first occurrence does not actually define the base of the *exaratum* Subzone, which is placed lower at the first occurrence of *Eleganticeras elegantulum* (Howarth, 1992; Fig. 2).

3. Materials and methods

3.1. Organic matter analysis: Carbon isotopes, TOC, S, N and SEM-EDX

Seventy-two mudstone and silty mudstone samples were analysed for bulk $\delta^{13}C_{org}$, which included a reanalysis of some samples originally analysed by Izumi et al. (2012). Powdered samples were decalcified in an excess of 3 M HCl, and then washed in milliQ water until neutrality was reached. Dried samples were weighed into Sn foil cups and analysed on an EA1110 elemental analyser linked to a Europa Scientific 2020 isotope ratio mass spectrometer. Analytical precision was better than 0.2‰ as determined by inter-run analysis of internal standards. One hundred twenty-two mudstone and silty mudstone samples were analysed for C, S and N abundance on a LECO CNS2000 elemental analyser. For total organic C (TOC) analysis, dried and powdered samples were weighed into ceramic boats and transferred to a furnace at 450 °C for 7–12 h prior to analysis in order to burn off all organic C. TOC was calculated by subtracting the total inorganic C content determined via this ashing procedure from the total C content determined from analysis of unashed sample. Inorganic C content was found to be negligible in most samples. Analytical precision for C and S was better than 0.03 wt.% (2σ) and 0.01 wt.% for N based on analysis of an in-house standard. Microscopic organic material was identified in samples using SEM imaging with element identification using EDX (energy dispersive X-ray) analysis. SEM-EDX analysis was carried out in backscatter mode using a dual beam FEI Quanta 200 3D microscope, online to an Oxford Instruments INCA energy dispersive X-ray detector.

3.2. Major and trace element analysis

One hundred seventeen mudstone and silty mudstone samples were analysed for major and trace element abundances using a Niton XL3t Goldd + portable XRF analyser. For these measurements, dried powdered samples were placed into 40 ml vials and covered with a non-PVC film. Up-turned vials were then placed on the X-ray aperture of the XRF instrument for analysis. Standardisation of elemental abundances was achieved by regression calibration to in-house standards. For the elements measured in this study (Ti, Rb, K, Zr, and Si) the calibration errors associated with these measurements were better than 0.03% for Ti, 0.22% for K, 6.69% for Si, 5.50 ppm for Rb, and 7.51 ppm for Zr. Accurate quantification of redox-sensitive V, Mo and Cr abundance was not possible using XRF owing to typically low abundances below the limit of detection of the instrument (in the case of Mo), or because of instrument limitations (in the case of V and Cr). For these elements, and also Al, ICP-AES analysis was carried out on a subset of 40 mudstone and silty mudstone samples. For ICP-AES analysis, 0.2 g of dried powdered sample was acid digested using a Multiwave 3000 (Anton Paar) digestion system in 8 ml of HNO_3. Filtered samples were analysed on a Thermo ICAP 6300 ICP-AES. Repeat analysis of standards yielded reproducibility for these elements of better than 3.45% RSD.

4. Results

4.1. Organic matter characterisation

The $\delta^{13}C_{org}$ excursion recognised by Izumi et al. (2012) has been reproduced here at higher resolution (72 samples versus 46 over the studied interval, Fig. 2). The data show consistent $\delta^{13}C_{org}$ values of ~ −25‰ from −17 m to ~−9 m. Above this, the onset of the early Toarcian $\delta^{13}C$ excursion is marked by a fall in $\delta^{13}C_{org}$ to ~−28.5‰. Patchy exposure in the Sakuraguchi-dani valley over this interval prevents the recovery of a detailed profile of the excursion onset (Fig. 2). The data do delineate, however, an abrupt, ~−2‰ shift in $\delta^{13}C_{org}$ values over 0.5 m (Fig. 2). Between ~−2 m and ~10 m, $\delta^{13}C_{org}$ is broadly consistent with values of ~−27.7‰. Above 10 m, $\delta^{13}C_{org}$ begins to increase, with values reaching ~−23.5‰ at ~30 m height (Fig. 2). Above this level, $\delta^{13}C_{org}$ shows a gradual decrease of ~−1‰ over the remaining ~25 m of the section (Fig. 2). As described above (Section 2), the pattern of carbon-isotope changes in the Sakuraguchi-dani succession is readily correlable with records from Northern Europe, notwithstanding the lack of detail close to the onset of the shift to more negative $\delta^{13}C_{org}$ values between ~−9 and ~−2 m (Fig. 2). In Fig. 3, TOC and TOC/N data are plotted alongside the $\delta^{13}C_{org}$ data. The TOC record through

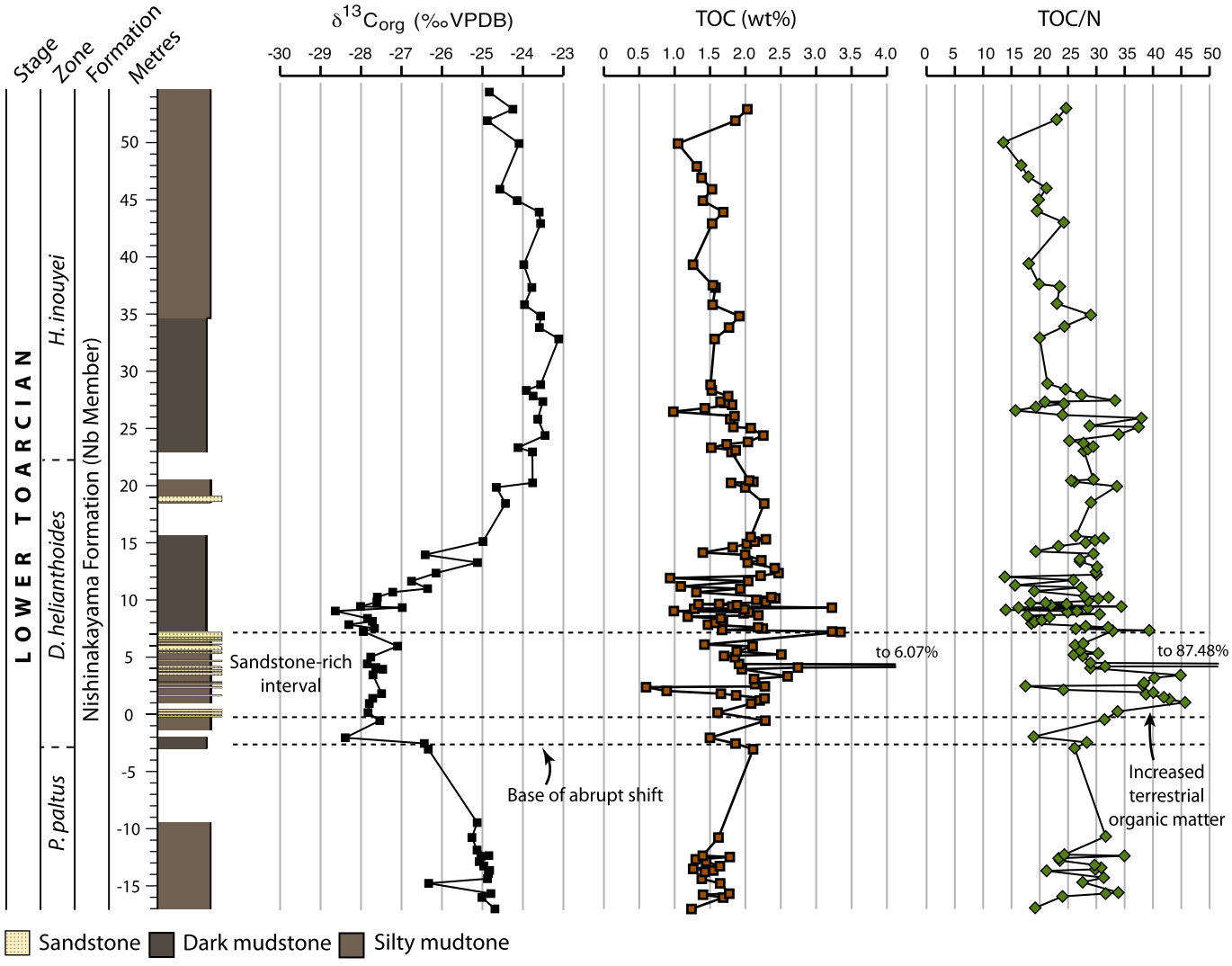

Fig. 3. TOC and TOC/N data through the Sakuraguchi-dani succession. $\delta^{13}C_{org}$ data also shown. Note the excursion in TOC/N between ~0 and ~3 m, suggestive of increased terrestrial organic matter flux (see Section 5.1 for discussion).

the Sakuraguchi-dani succession indicates pervasive but variable organic matter enrichment through the succession, with a mean TOC of 1.85%. Highest TOC abundances are reached in the *Dactylioceras helianthoides* Zone (~0 to ~7 m, Fig. 3), broadly within the interval of minimum $\delta^{13}C_{org}$ values. Our higher-resolution record contrasts with the TOC record of Izumi et al. (2012), who recognised a lowering of TOC coincident with the sandstone-rich interval in the *D. helianthoides* Zone between ~0 and ~7.3 m. Izumi et al. (2012) suggested a predominantly terrestrial origin for the organic matter in the Sakuraguchi-dani succession owing to the generally high $\delta^{13}C_{org}$ values relative to marine dominated records of the event (e.g. Yorkshire, UK, Fig. 2), and the common occurrence of macroscopic wood in the section (e.g. Izumi et al., 2012). Here, SEM-EDX analysis also confirms the presence of tabular wood fragments at the microscopic (i.e. ≪1 mm) scale (Fig. 4). TOC/N ratios can potentially be used as a proxy for organic matter source on the basis that vascular land plants typically have TOC/N >20, whereas algal organic matter of marine origin usually has TOC/N <10 (e.g. Meyers, 1997). Mean TOC/N in the section is 27.46, supporting the other inferences regarding the predominance of terrestrial organic matter. In detail, TOC/N variations show a similar pattern to TOC through the succession, but with a pronounced increase to values of ~40 between ~0 and ~3 m (Fig. 3).

4.2. Detrital proxies

Elements such as Al, Ti, Zr, Si, Rb, and K are associated with terrigenous mineral phases and thus potentially are able to provide insights into the nature of detrital (i.e. eolian and fluvial) fluxes in marine mudrocks. Relative changes in the abundance of Ti and Zr have also been used previously as grain size proxies owing to the expected enrichment of these elements in silt to sand sized sediment relative to their abundance in clay minerals (notwithstanding the presence of clay-bound Ti, for example) (Calvert and Pedersen, 2007). The relatively high density of minerals rich in these elements, such as zirconium ($ZrSiO_4$), rutile (TiO_2) and ilmenite ($FeTiO_3$), means that these elements are commonly transported with silt and sand-sized quartz in the detrital fraction, leading to a grain-size association (Spears and Kanaris-Sotiriou, 1976; Chen et al., 2006; Calvert and Pedersen, 2007). In contrast, K is most strongly associated with aluminosilicates such as clay minerals (e.g. illite), and due to ionic size similarities Rb readily substitutes for K leading to a strong association between the two elements (Calvert and Pedersen, 2007). Abundances of Ti, Rb, Zr, Si and K measured using XRF and normalised to ICP-AES determined Al in the mudstone and silty mudstone facies of the succession show similar trends (Fig. 5). Notably, the proxies all show a pronounced increase between ~7.3 m and ~13.5 m, coincident with the most rapid recovery phase of the $\delta^{13}C_{org}$ signal (Fig. 5). The correspondence between the Al-normalised data suggests a common detrital source for the analysed elements. However, a high co-efficient of variation for Al in the succession relative to the other element abundances indicates that this correspondence is dependent, at least in part, on the strong Al variability (see, for example, Van der Weijden, 2002). Directly comparing the elemental ratio of coarse-grained proxies (Ti, Zr) relative to clay proxies (K, Rb) allows a potentially more informative assessment of the nature of the detrital flux. Specifically, K/Ti and Rb/Zr ratios show an approximate correspondence to changing facies through the section (Fig. 5); with a pronounced decrease in values at ~0 m coincident with the change to a silty facies with intercalated sandstones (note from Section 3.2 that no sandstone samples were analysed). Minimum K/Ti and Rb/Zr values are reached at ~3 m, followed by a rise in values up to ~7 m, whereupon the rock type becomes a finer grained dark mudstone (Fig. 5). Maximum Rb/Zr and K/Ti values are reached in the dark mudstone facies between ~8 and ~14 m, before falling to generally consistent values over the remainder of the succession (Fig. 5).

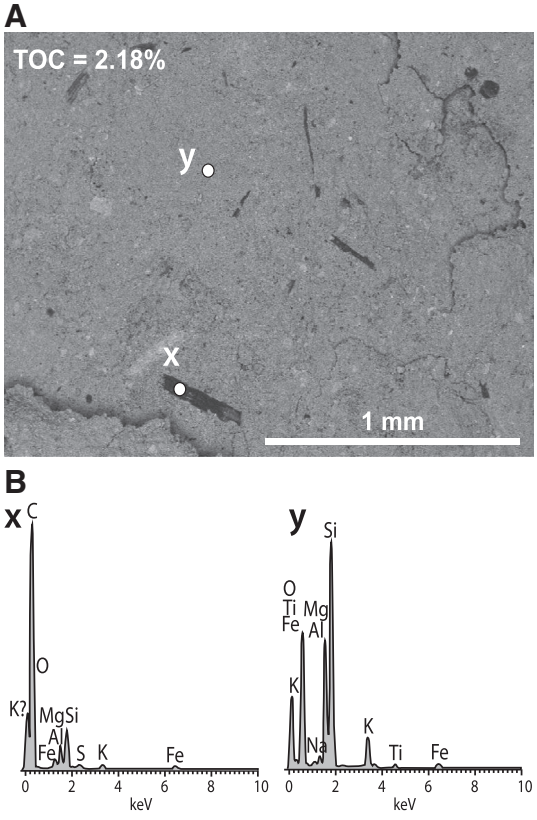

Fig. 4. A. Backscatter SEM image of Sakuraguchi-dani sample (sample positioned at ~7 m height, Fig. 2). TOC of the sample is 2.18%. Note presence of dark, tabular sub-millimetre wood fragments. B. EDX analysis of these fragments compared to rock groundmass indicates high carbon content consistent with this interpretation.

4.3. Palaeoredox proxies

Izumi et al. (2012) presented an ichnofabric analysis of the Sakuraguchi-dani section that indicated the ephemeral occurrence of laminated and unbioturbated facies (ichnofabric index of 1 or 2, Fig. 6) through the succession, most notably from the middle part of the *Dactylioceras helianthoides* Zone (~10 m, Fig. 6) to partway through the *Harpoceras inouyei* Zone (~40 m, Fig. 6). These authors suggested that this intermittent lack of bioturbation, coupled with generally high TOC values through the succession, was most likely a result of deposition under suboxic/anoxic conditions (Izumi et al., 2012). The large swings observable in the ichnofabric index data argue for a lack of sustained anoxia and frequent reoxygenation (Fig. 6; Izumi et al., 2012). The solubility of Mo is lowered under reducing conditions, thus promoting sedimentary burial (e.g. Algeo and Lyons, 2006). However, Mo abundance in the Sakuraguchi-dani succession (mean = 0.37 ppm) is below average for typical shale concentrations (c. 1 ppm, Wedepohl, 1991; Fig. 6). [Mo] and Mo/TOC values show an increase between ~8 and 11 m, coincident with the shift to more positive $\delta^{13}C_{org}$ values and the clay-rich facies as inferred from K/Ti and Rb/Zr ratios (Fig. 5). This increase is not accompanied by an increase in TOC, however. Indeed, Mo and TOC do not correlate in the succession (Fig. 7A). Trends in V/Al and Cr/Al are similar, and differ markedly from the [Mo] and Mo/TOC trends (Fig. 6). Highest V/Al and Cr/Al occur broadly coeval with the sandstone-rich interval (~0 to 7.3 m) and below the peaks in Mo abundance. As with [Mo], V/Al and Cr/Al abundances are not anomalously high in the succession relative to average shale values (Wedepohl, 1991; Fig. 6). Moreover, there is a clear correlation of Cr and V with Al abundance, which indicates a predominantly detrital, rather than redox, control on the abundance of these elements (Fig. 7B and C; Jones and Manning, 1994; Tribovillard et al., 2006). Pyrite is a readily observable component of the sediments (Tanabe et al., 1984 and field

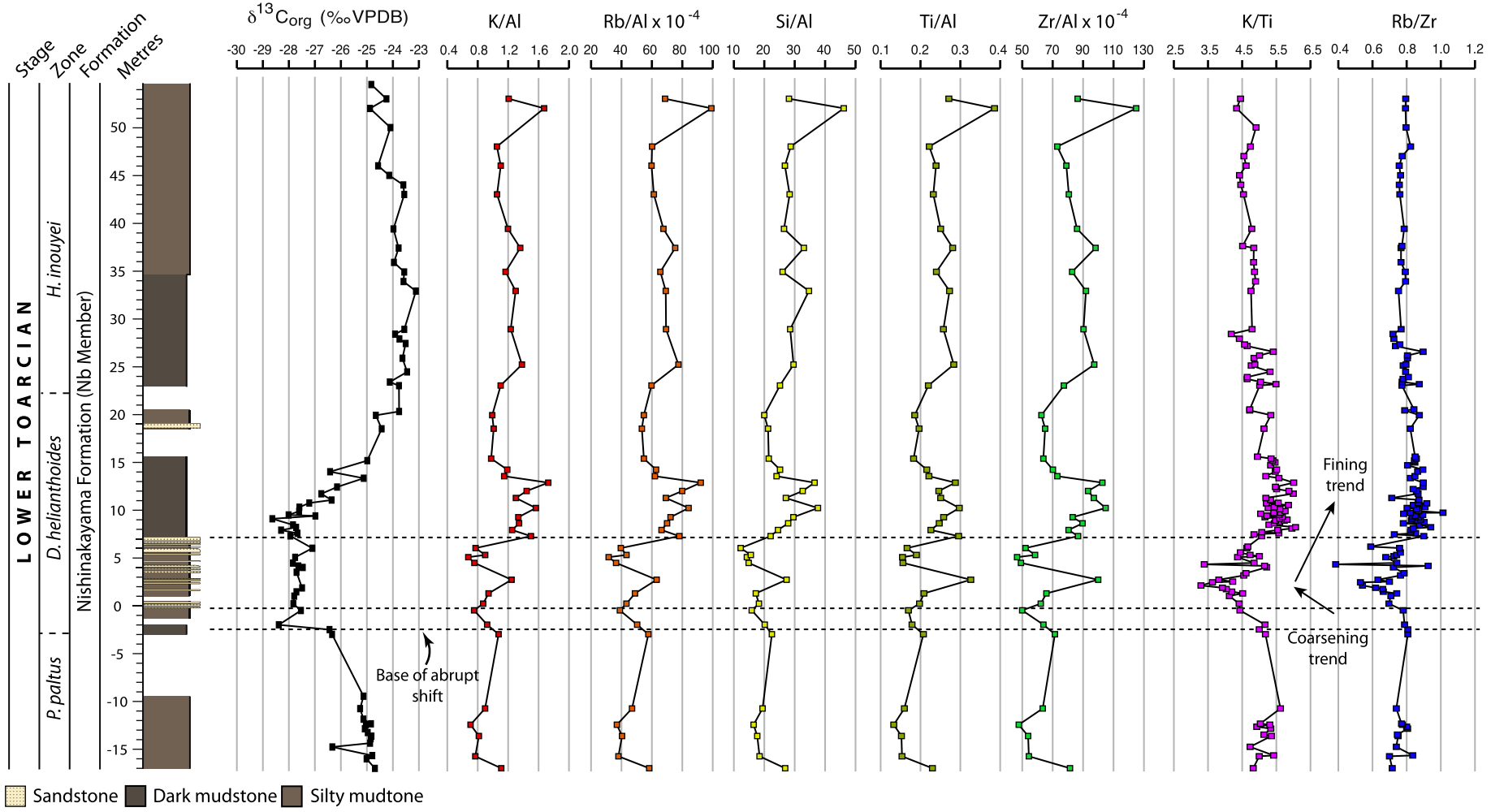

Fig. 5. Stratigraphic distribution of detrital major and trace element proxies in the Sakuraguchi-dani succession. Note the common behaviour of Al normalised elements, and the clear trends in K/Ti and Rb/Zr grain size proxies.

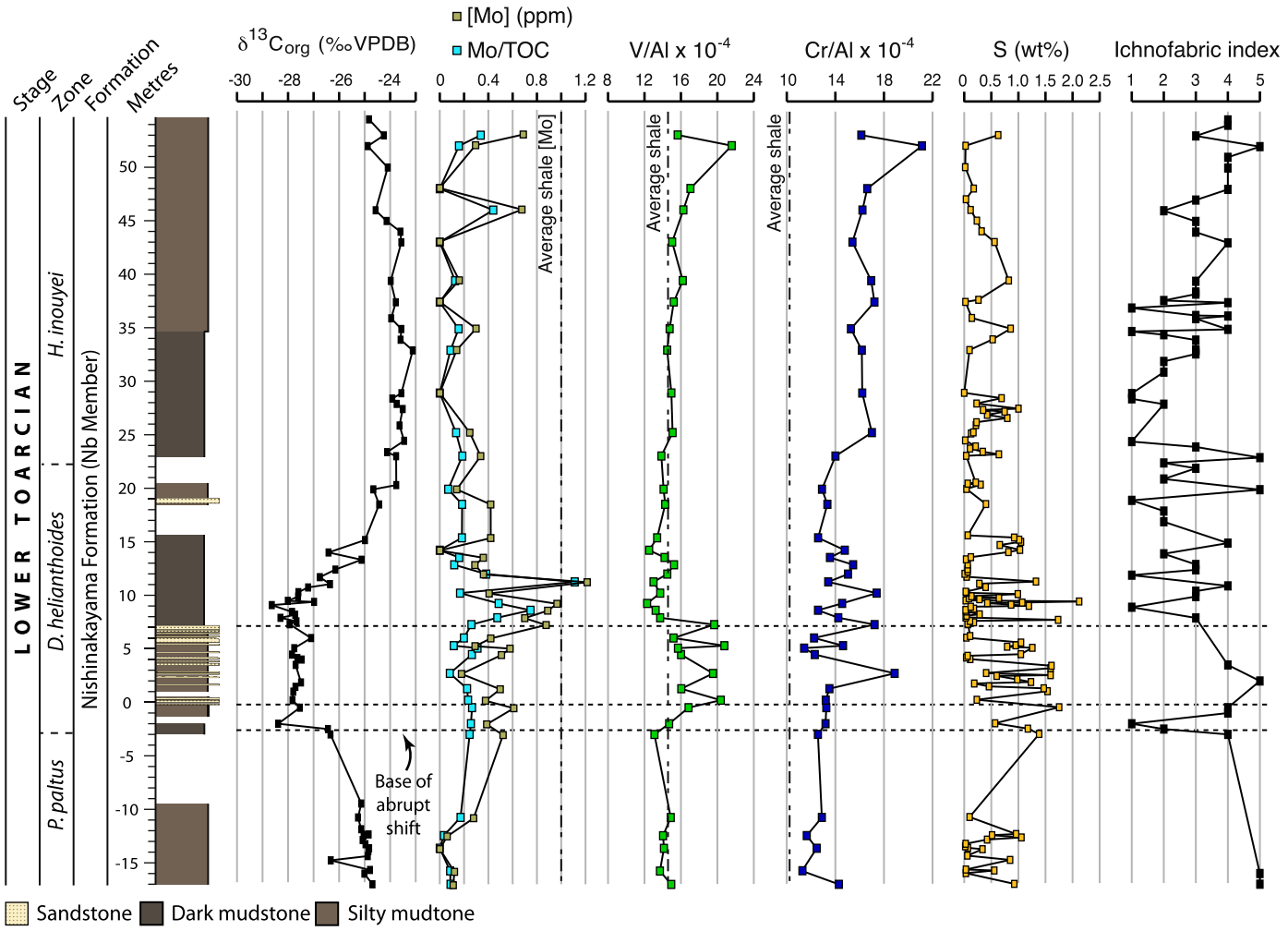

Fig. 6. Stratigraphic distribution of redox-sensitive elemental data in the Sakuraguchi-dani succession. Note the lack of correspondence between the various proxies, notably [Mo] and Mo/TOC and ichnofabric index. S is assumed to be present predominantly in the form of pyrite. Average shale values are from Wedepohl (1991). Ichnofabric index data are from Izumi et al. (2012): 1 = no bioturbation, well laminated, 2 = weak bioturbation, laminated, 3 = bioturbated, poorly laminated, 4 = bioturbated, few laminations, 5 = well bioturbated, not laminated (see Droser and Bottjer, 1986 for original definitions).

observations), and assuming this is the only S-bearing mineral in the succession (as suggested by XRD results in Izumi, 2014), the S data potentially provide insights into redox controlled pyrite distribution and abundance (Fig. 6). Fig. 6 indicates that S is highly variable (mean = 0.48%), and does not have an obvious correlation to the ichnofabric index, or a statistically significant correlation with TOC (Fig. 7D). Generally elevated S abundance occurs between ~−3 and ~5 m, but clear trends in the data are not otherwise apparent. S content is zero in parts of the succession (Fig. 6), indicating an absence of pyrite at various horizons regardless of the veracity of the assumption that pyrite represents the only S-bearing mineral phase.

5. Discussion

5.1. Sedimentological and geochemical changes in the Sakuraguchi-dani succession and possible links to palaeoenvironmental change

Variations in K/Ti and Rb/Zr through the Sakuraguchi-dani succession are suggestive of marked changes in the nature of the sediment flux in the succession. These changes are broadly aligned with facies changes and one interpretation is that they reflect the consequences of variations in relative sea level. A fall in relative sea level close to the initial shift to more negative $\delta^{13}C_{org}$ values at or just below ~0 m is supported by the decrease in K/Ti and Rb/Zr, reflecting a coarsening of the mudrock facies that is also coincident with the first occurrence of intercalated sandstone beds in the succession (Fig. 5). Kawamura (2010) previously interpreted these sandstone horizons in this part of the Nishinakayama succession as turbiditic event beds with Bouma-type facies motifs. Both sediment coarsening and the onset of gravity-driven sediment deposition could have arisen from deposition within a more proximal setting coupled with enhanced fluvial incision and shelf instability resulting from forced regression. In addition, low values of K/Ti and Rb/Zr are broadly coincident with maximum TOC/N values between ~0 and ~3 m (Figs. 3 and 5). This increase in TOC/N likely reflects an increase in the relative abundance of terrestrial organic matter versus marine organic matter (see Section 4.1), which could represent a further consequence of deposition in a more proximal marine setting. The rise in K/Ti and Rb/Zr from ~3 m to 10 m, coincident with a general decrease in TOC/N, could similarly be interpreted as a transgressive fining up signature (Figs. 3 and 5).

Sequence stratigraphic analysis of European basins has provided evidence for sea-level fall close to the onset of the early Toarcian $\delta^{13}C$ excursion (Perilli, 2000; Wignall et al., 2005; Pittet et al., 2014). Notably, in the Cleveland Basin (UK) a short-lived interval of hummocky cross-stratification development occurs close to the top of the *tenuicostatum* Zone below the first abrupt negative shift in $\delta^{13}C_{org}$ (Wignall et al., 2005; Fig. 2). In the Lusitanian Basin (Portugal), there is similar evidence for sea-level fall n the upper *tenuicostatum* Zone in the form of a regional hiatus that occurs immediately prior to the onset of the early Toarcian $\delta^{13}C$ excursion (Pittet et al., 2014). This has been interpreted as a

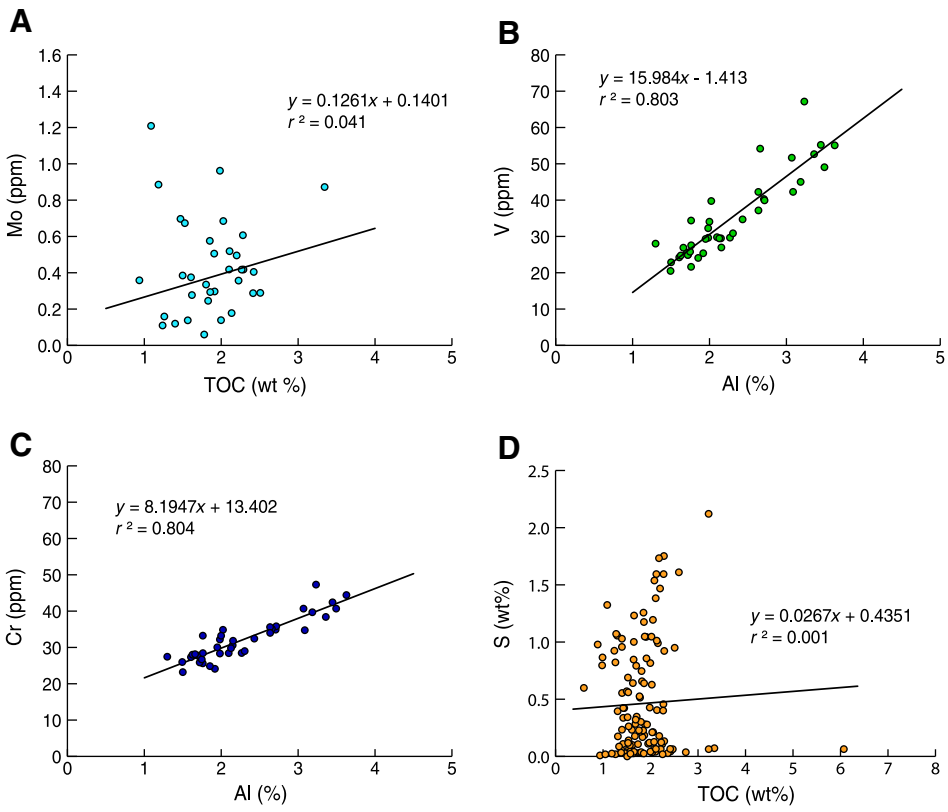

Fig. 7. Cross-plots of elemental and organic geochemical data, and associated linear regression correlation statistics. The cross plots of Cr and V with Al indicate a strong detrital control on the abundance of these elements. Note the lack of correlation between TOC and S, and Mo and TOC.

potentially glacioeustatic event (Pittet et al., 2014). In the Sakuraguchi-dani succession, the geochemical evidence for sea-level fall slightly post-dates the onset of the negative $\delta^{13}C$ excursion (Fig. 5), contrasting with the evidence from the Lusitanian and Cleveland basins. Indeed, the onset of the $\delta^{13}C$ excursion in the Lusitanian Basin is associated with sediment starvation and inferred transgression (Pittet et al., 2014). Evidence from other European and Arctic basins also indicates strongly transgressive conditions through the early Toarcian (e.g. Hallam, 1997, 2001; Nikitenko and Mickey, 2004; Hesselbo, 2008; Hermoso et al., 2013). Localised sea-level changes in the Tabe Basin could have driven the observed changes, with the position of the basin in the Early Jurassic within a convergent island arc setting supporting the likely importance of tectonic controls on basin development (e.g. Taira et al., 1983). An alternative hypothesis for the observed facies changes, however, arises from the prominent palaeoenvironmental changes that also punctuated the interval, which could have led to climatically mediated changes in sediment supply (Hesselbo et al., 2007; Hesselbo, 2008). Notably, the geochemically inferred coarsening, initiation of sandstone turbidites, and elevated TOC/N values occur just above the onset of the $\delta^{13}C$ excursion (Figs. 3 and 5), where a global increase in weathering and hydrological cycling under elevated temperatures and pCO_2 has been inferred on the basis of geochemical evidence from European sections (Bailey et al., 2003; Cohen et al., 2004; McElwain et al., 2005; Dera et al., 2009). Hesselbo et al. (2007) noted a very similar coincidence between the occurrence of turbidite and debris flow deposits and $\delta^{13}C$ changes from an early Toarcian section exposed in Peniche, Portugal. In both the Sakuraguchi-dani and Peniche sections, gravity flow deposits first occur immediately above the onset of the negative $\delta^{13}C$ excursion, and decrease markedly in abundance when the $\delta^{13}C$ signals start to recover to more positive values (cf. Hesselbo et al., 2007 and Fig. 2). Hesselbo et al. (2007) suggested that a climatically forced increase in erosion rates and hence sediment supply could account for the observed facies changes in the Peniche section, and by extension the same mechanism could account for the changes observable in the Sakuraguchi-dani succession. The start and end of the negative $\delta^{13}C$ excursion is coincident with an Os-isotope excursion recorded from the Cleveland Basin of Yorkshire, UK, that has been interpreted to reflect a 4- to 8-fold increase in global chemical weathering rates (Cohen et al., 2004). The onset of this increase is coeval with a calculated 6–7 °C increase in seawater temperatures based on belemnite $\delta^{18}O$ and Mg/Ca from the same succession (McArthur et al., 2000; Bailey et al., 2003; see also Dera et al., 2009). The utility of this Os-isotope record for assessing global weathering has since been questioned (Waltham and Gröcke, 2006; McArthur et al., 2008), but additional geochemical evidence supports the inference of accelerated rates of hydrological cycling, and thus likely elevated fluvial sediment supply, during the early Toarcian event. In particular, Dera et al. (2009) assessed the Europe-wide distribution of clay minerals through the late Pliensbachian and early Toarcian and recognised that significant kaolinite enrichment occurs within the *falciferum* Zone, broadly coeval (within the resolution of the analysis) with the $\delta^{13}C$ excursion. This relative increase in kaolinite abundance was interpreted as evidence for highly efficient continental runoff under a warm, humid climate state (Dera et al., 2009).

5.2. Palaeoredox changes in the Sakuraguchi-dani succession

The relatively high TOC values and ichnofabric data of Izumi et al. (2012) support the inference that seawater deoxygenation was an important feature of the Sakuraguchi-dani succession. Nevertheless, the ephemeral occurrence of unlaminated and bioturbated strata in the succession, and the lack of clear evidence for anoxia from the elemental palaeoredox proxies presented here, argue against pervasive anoxic conditions (Fig. 6). Analyses of Panthalassic pelagic cherts (exposed in Japan on accreted terranes and thus not necessarily palaeogeographically proximal to the Toyora area rocks) suggest that more pervasive seawater

deoxygenation was a feature of the deeper northwest Panthalassa Ocean through the early Toarcian (Wignall et al., 2010; Sato et al., 2012). The relatively shallow nature of the Tabe Basin could have prevented the development of a permanent chemocline, with recurrent, seasonally controlled, oxygenation of the basin. Variable rates of sedimentation may have played a key role in influencing the development of the various ichnofabrics recognised by Izumi et al. (2012), and indeed the relative enrichment of authigenic mineral phases, such as Mo (Fig. 6). Certainly, Mo concentrations in the section, if predominantly authigenic in origin, perhaps better reflect changing sediment flux, hence leading to the relative enrichment between ~8 and 11 m, where clay-rich facies dominate, and where the two peaks delineated in [Mo] and Mo/TOC at ~9 m and ~11 m are coeval with ichnofabrics of 1 (i.e. well-laminated and lacking any bioturbation, Fig. 6). Elsewhere in the succession a link between geochemically inferred grain size and ichnofabric index is not apparent, and thus substrate composition was unlikely to have been a primary control on ichnofabric development, suggesting instead that observed changes in ichnofacies reflect primarily redox control (Izumi et al., 2012). The organic matter enrichment of the Sakuraguchi-dani succession is notable in the context of the overall thickness of the $\delta^{13}C_{org}$ excursion interval, which spans ~40 m (Fig. 2). This is similar to the thickness of the excursion in Peniche, Portugal, where terrestrial organic matter enrichment is substantially lower (average TOC ~0.5%; Hesselbo et al., 2007). Thus, a far higher flux of organic matter must have persisted throughout deposition of the Sakuraguchi-dani succession. Although the preservation potential of this organic matter must have remained similarly high throughout deposition, the terrestrial origin suggests that organic carbon enrichment was likely highly dependent on the terrigenous flux, in addition to any relevant redox factors, potentially accounting for the lack of correlation of TOC with authigenic S and Mo.

6. Conclusions

We have presented the first multiproxy geochemical analysis of a Panthalassic margin record of the early Toarcian oceanic anoxic event. Our data demonstrate little evidence for the development of pervasive anoxia on the northwestern Panthalassa shelf, though high levels of terrestrial organic matter and intermittent well-laminated horizons support at least ephemeral deoxygenation and high organic carbon preservation potential. Analysis of detrital elemental proxies and gravity driven deposits through the succession indicate facies changes that correlate at least in part with $\delta^{13}C$ changes. In the context of the major global climatic changes that occurred during the early Toarcian and similar early Toarcian facies changes previously recognised in Portugal, it is possible that these changes in detrital sediment flux may have arisen as a direct consequence of accelerated hydrological cycling under warmer climatic conditions.

Acknowledgements

DBK acknowledges receipt of NERC Fellowship NE/I01089X/1. KI was funded through a grant from JSPS (24-8818). The authors acknowledge the help of Masayuki Ikeda during fieldwork, and the help of Yasuhiro Ito for housing the rock samples in The University Museum, University of Tokyo (UMUT). Diane Johnson is thanked for assistance with SEM imaging. The authors thank Silvia Danise, Marie-Emile Clémence, Kazushige Tanabe, and Kentaro Nakada for helpful discussions. The comments of two anonymous reviewers greatly improved the manuscript.

Appendix A. Supplementary data

Supplementary data to this article can be found online at http://dx.doi.org/10.1016/j.palaeo.2014.09.019.

References

Algeo, T.J., Lyons, T.W., 2006. Mo-total organic carbon covariation in modern anoxic marine envrionments: implications for analysis of paleoredox and paleohydrographic conditions. Palaeoceanography 21. http://dx.doi.org/10.1029/2004PA001112.

Al-Suwaidi, A.H., Angelozzi, G.N., Baudin, F., Damborenea, S.E., Hesselbo, S.P., Jenkyns, H.C., Mancenido, M.O., Riccardi, A.C., 2010. First record of the Early Toarcian oceanic anoxic event from the Southern Hemisphere, Neuquén Basin, Argentina. J. Geol. Soc. Lond. 167, 633–636.

Bailey, T.R., Rosenthal, Y., McArthur, J.M., van de Schootbrugge, B., Thirlwall, M.F., 2003. Paleoceanographic changes of the Late Pliensbachian–early Toarcian interval: a possible link to the genesis of an Oceanic Anoxic Event. Earth Planet. Sci. Lett. 212, 307–320.

Calvert, S.E., Pedersen, T.F., 2007. Elemental proxies for palaeoclimatic and palaeoceanographic variability in marine sediments: interpretation and application. In: Hillaire-Marcel, C., Vernal, A.D. (Eds.), Proxies in Late Cenozoic Paleoceanography. Elsevier, Amsterdam, pp. 567–644.

Caruthers, A.H., Gröcke, D.R., Smith, P.L., 2011. The significance of an Early Jurassic (Toarcian) carbon-isotope excursion in Haida Gwaii (Queen Charlotte Islands). British Columbia Canada. Earth Planet. Sci. Lett. 307, 19–26.

Caswell, B.A., Coe, A.L., Cohen, A.S., 2009. New range data for marine invertebrate species across the early Toarcian (Early Jurassic) mass extinction. J. Geol. Soc. Lond. 166, 859–872.

Chen, J., Chen, Y., Liu, L., Ji, J., Balsam, W., Sun, Y., Lu, H., 2006. Zr/Rb ratio in the Chinese loess sequences and its implication for changes in the East Asian winter monsoon strength. Geochim. Cosmochim. Acta 70, 1471–1482.

Cohen, A.S., Coe, A.L., Harding, S.M., Schwark, L., 2004. Osmium isotope evidence for the regulation of atmospheric CO_2 by continental weathering. Geology 32, 157–160.

Danise, S., Twichett, R.J., Little, C.T.S., Clemence, M.-E., 2013. The impact of global warming and anoxia on marine benthic community dynamics: an example from the Toarcian (Early Jurassic). Plos One http://dx.doi.org/10.1371/journal.pone.0056255.

Dera, G., Pellenard, P., Niege, P., Deconinck, J.-F., Puceat, E., Dommergues, J.-L., 2009. Distribution of clay minerals in Early Jurassic peritethyan seas: palaeoclimatic significance inferred from multiproxy comparisions. Palaeogeogr. Palaeoclimatol. Palaeoecol. 271, 39–51.

Droser, M.L., Bottjer, D.J., 1986. A semiquantitative field classification of ichnofabric. J. Sediment. Petrol. 59, 558–559.

French, K.L., Sepúlveda, J., Trabucho-Alexandre, J., Gröcke, D.R., Summons, R.E., 2014. Organic geochemistry of the early Toarcian oceanic anoxicevent in Hawsker Bottoms, Yorkshire, England. Earth Planet. Sci. Lett. 390, 116–127.

Gröcke, D.R., Hori, R.S., Trabucho-Alexandre, J., Kemp, D.B., Schwark, L., 2011. An open marine record of the Toarcian oceanic anoxic event. Solid Earth 2, 245–257. http://dx.doi.org/10.5194/se-2-245-2011.

Hallam, A., 1997. Estimates of the amount and rate of sea-level change across the Rhaetian-Hettangian and Pliensbachian-Toarcian boundaries (latest Triassic to early Jurassic). J. Geol. Soc. Lond. 154, 773–779.

Hallam, A., 2001. A review of the broad pattern of Jurassic sea-level changes and their possible causes in the light of current knowledge. Palaeogeogr. Palaeoclimatol. Palaeoecol. 167, 23–37.

Hermoso, M., Minoletti, F., Pellenard, P., 2013. Black shale deposition during the Toarcian super-greenhouse driven by sea-level. Clim. Past 9, 2703–2712. http://dx.doi.org/10.5194/cp-9-2703-2013.

Hesselbo, S.P., 2008. Sequence stratigraphy and inferred relative sea-level change from the onshore British Jurassic. Proc. Geol. Assoc. 119, 19–34.

Hesselbo, S.P., Gröcke, D.R., Jenkyns, H.C., Bjerrum, C.J., Farrimond, P., Morgans Bell, H.S., Green, O.R., 2000. Massive dissociation of gas hydrate during a Jurassic oceanic event. Nature 406, 392–395.

Hesselbo, S.P., Jenkyns, H.C., Duarte, L.V., Oliveira, L.C.V., 2007. Carbon-isotope record of the Early Jurassic (Toarcian) Oceanic Anoxic Event from fossil wood and marine carbonate (Lusitanian Basin, Portugal). Earth Planet. Sci. Lett. 253, 455–470.

Hirano, H., 1973. Biostratigraphic study of the Jurassic Toyora Group, part 3. Transactions and Proceedings of the Palaeontological Society of Japan, New Series 90, pp. 45–71.

Howarth, M.K., 1992. The Ammonite family Hildoceratidae in the Lower Jurassic of Britain. Monogr. Palaeontol. Soc. 2 107–200.

Izumi, K., 2014. Utility of geochemical analysis of trace fossils: case studies using *Phycosiphon incertum* from the Lower Jurassic shallow-marine (Higashinagano Formation, southwest Japan) and Pliocene deep-marine deposits (Shiramazu Formation, central Japan). Ichnos 21, 62–72.

Izumi, K., Miyaji, T., Tanabe, K., 2012. Early Toarcian (Early Jurassic) oceanic anoxic event recorded in the shelf deposits in the northwestern Panthalassa: evidence from the Nishinakayama Formation in the Toyora area, west Japan. Palaeogeogr. Palaeoclimatol. Palaeoecol. 315–316, 100–108.

Jenkyns, H.C., 1988. The early Toarcian (Jurassic) anoxic event—stratigraphic, sedimentary, and geochemical evidence. Am. J. Sci. 288, 101–151.

Jenkyns, H.C., Gröcke, D.R., Hesselbo, S.P., 2001. Nitrogen isotope evidence for water mass denitrification during the early Toarcian (Jurassic) oceanic anoxic event. Palaeoceanography 16, 593–603.

Jones, B., Manning, D.A.C., 1994. Comparison of geochemical indices used for the interpretation of palaeoredox conditions in ancient mudstones. Chem. Geol. 111, 111–129.

Kafousia, N., Karakitsios, V., Jenkyns, H.C., Mattioli, E., 2011. A global event with a regional character: the Early Toarcian Oceanic Anoxic Event in the Pindos Ocean (northern Peloponnese, Greece). Geol. Mag. 148 (4), 619–631.

Kawamura, H., 2010. Stratigraphic revision of the Jurassic Toyora Group of the southern part of the Tabe Basin, Yamaguchi Prefecture, southwest Japan. J. Geol. Soc. Jpn. 116 (1), 27–44.

Kemp, D.B., Coe, A.L., Cohen, A.S., Schwark, L., 2005. Astronomical pacing of methane release in the Early Jurassic period. Nature 437, 396–399.
Matsumoto, T., Ono, A., 1947. A biostratigraphic study of the Jurassic Toyora Group, with special reference to ammonites. Science Reports of the Faculty of Science, Kyusha University. Geology 2, 20–31.
Mazzini, A., Svensen, H., Leanza, H.A., Corfu, F., Planke, S., 2010. Early Jurassic shale chemostratigraphy and U–Pb ages from the Neuquén Basin (Argentina): implications for the Toarcian Oceanic Anoxic Event. Earth Planet. Sci. Lett. 297, 633–645.
McArthur, J.M., Donovan, D.T., Thirlwall, M.F., Fouke, B.W., Mattey, D., 2000. Strontium isotope profile of the early Toarcian (Jurassic) oceanic anoxic event, the duration of ammonite biozones, and belemnite palaeotemperatures. Earth Planet. Sci. Lett. 179, 269–285.
McArthur, A.G., Algeo, T.J., van de Schootbrugge, B., Li, Q., Howarth, R.J., 2008. Basinal restriction, black shales, Re–Os dating, and the Early Toarcian (Jurassic) oceanic anoxic event. Paleoceanography 23, PA4217. http://dx.doi.org/10.1029/2008PA001607.
McElwain, J.C., Wade-Murphy, J., Hesselbo, S.P., 2005. Changes in carbon dioxide during an oceanic anoxic event linked to intrusion into Gondwana coals. Nature 435 (7041), 479–482.
Meyers, P.A., 1997. Organic geochemical proxies of paleoceanographic, palaeolimnologic, and paleoclimatologic processes. Org. Geochem. 27, 213–250.
Nakada, K., Matsuoka, A., 2011. International correlation of the Pliensbachian/Toarcian (Lower Jurassic) ammonoid biostratigraphy of the Nishinakayama Formation in the Toyora Group, southwest Japan. Newsl. Stratigr. 44, 89–111.
Nikitenko, B.L., Mickey, M.B., 2004. Foraminifera and ostracodes across the Plensbachian-Toarcian boundary in the Arctic Realm (stratigraphy, palaeobiogeography and biofacies). In: Beaudoin, A.B., Head, M.J. (Eds.), Geological Society, London, Special Publications 230, pp. 137–174.
Page, K.N., 2003. The Lower Jurassic of Europe: its subdivision and correlation. Geol. Surv. Den. Greenl. Bull. 1, 23–59.
Perilli, N., 2000. Calibration of early–middle Toarcian nannofossil events based on high-resolution ammonite biostratigraphy in two expanded sections from the Iberian Range (East Spain). Mar. Micropaleontol. 39, 293–308.
Pittet, B., Suan, G., Lenoir, F., Duarte, L.V., Mattioli, E., 2014. Carbon isotope evidence for sedimentary discontinuities in the lower Toarcian of the Lusitanian Basin (Portugal): sea level change at the onset of the Oceanic Anoxic Event. Sediment. Geol. 303, 1–14.
Sato, T., Isozaki, Y., Shozugawa, K., Seimiya, K., Matsuo, M., 2012. ^{57}Fe Mössbauer analysis of the Upper Triassic–Lower Jurassic deep-sea chert: paleo-redox history across the Triassic–Jurassic boundary and the Toarcian oceanic anoxic event. Hyperfine Interact. 208, 95–98. http://dx.doi.org/10.1007/s10751-011-0520-4.
Schmidt-Effing, R., 1972. Die Dactylioceratidae, eine Ammoniten-Familie des unteren Jura. Münstersche Forschungen zur Geologie und Paläontologie, (173 pp.).
Spears, D.A., Kanaris-Sotiriou, R., 1976. Titanium in some Carboniferous sediments from Great Britain. Geochim. Cosmochim. Acta 40, 345–351.
Svensen, H., Planke, S., Chevallier, L., Malthe-Sorenssen, A., Corfu, F., Jamtveit, B., 2007. Hydrothermal venting of greenhouse gases triggering Early Jurassic global warming. Earth Planet. Sci. Lett. 256, 554–566.
Taira, A., Saito, Y., Hashimoto, M., 1983. The role of oblique subduction and strike-slip tectonics in the evolution of Japan. In: Hilde, T.W.C., Uyeda, S. (Eds.), Geodynamics of the Western Pacific-Indonesian Region. American Geophysical Union, Washington, D. C. http://dx.doi.org/10.1029/GD011p0303.
Tanabe, K., Inazumi, A., Ohtsuka, Y., Katsuta, T., Tamahama, K., 1982. Litho- and biofacies and chemical composition of the Lower Jurassic Nishinakayama Formation (Toyora Group) in West Japan. Memoirs of Ehime University, Series D (Earth Science) 9, pp. 47–62 (in Japanese with English abstract).
Tanabe, K., Inazumi, A., Tamahama, K., Takashi, K., 1984. Taphonomy of half and compressed ammonites from the lower Jurassic black shales of the Toyora area, west Japan. Palaeogeogr. Palaeoclimatol. Palaeoecol. 47, 329–346.
Trecalli, A., Spangenberg, J., Adatte, T., Follmi, K.B., Parente, M., 2012. Carbonate platform evidence of ocean acidification at the onset of the early Toarcian oceanic anoxic event. Earth Planet. Sci. Lett. 357–358, 214–225.
Tribovillard, N., Algeo, T.J., Lyons, T., Riboulleau, A., 2006. Trace metals as paleoredox and paleoproductivity proxies: an update. Chem. Geol. 232, 12–32.
Van der Weijden, C.H., 2002. Pitfalls of normalization of marine geochemical data using a common divisor. Mar. Geol. 184, 167–187.
Von Hillebrandt, A., Schmidt-Effing, R., 1981. Ammoniten aus dem Toarcium (Jura) von Chile (Südamerika). Zitteliana 6, 3–74.
Waltham, D., Gröcke, D.R., 2006. Non-uniqueness and interpretation of the seawater $^{87}Sr/^{86}Sr$ curve. Geochim. Cosmochim. Acta 70, 384–394.
Wedepohl, K.H., 1991. The composition of the upper Earth's crust and the natural cycles of selected metals. In: Merian, E. (Ed.), Metals and their Compounds in the Environment. Weinheim, VCH-Verlagsgesellschaft, pp. 3–17.
Wignall, P.B., Newton, R.J., Little, C.T.S., 2005. The timing of paleoenvironmental change and cause-and-effect relationships during the Early Jurassic mass extinction in Europe. Am. J. Sci. 305, 1014–1032.
Wignall, P.B., Bond, D.P.G., Kuwahara, K., Kakuwa, Y., Newton, R.J., Poulton, S.W., 2010. An 80 million year oceanic redox history from Permian to Jurassic pelagic sediments of the Mino-Tamba terrane, SW Japan, and the origin of four mass extinctions. Glob. Planet. Chang. 71, 109–123.